RESEARCH ARTICLE | JUNE 29 2020

Quantum confinement of coherent acoustic phonons in transferred single-crystalline bismuth nanofilms

Feng He ; Emily S. Walker; Yongjian Zhou; Sarah E. Muschinske; Seth R. Bank; Yaguo Wang

Appl. Phys. Lett. 116, 263101 (2020)
https://doi.org/10.1063/5.0007168
CHORUS

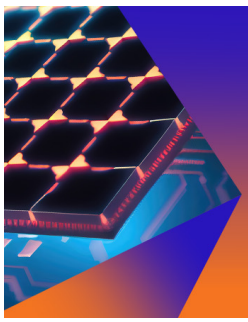

Applied Physics Letters ARTICLE scitation.org/journal/apl

Quantum confinement of coherent acoustic phonons in transferred single-crystalline bismuth nanofilms

Cite as: Appl. Phys. Lett. **116**, 263101 (2020); doi: 10.1063/5.0007168
Submitted: 10 March 2020 · Accepted: 13 June 2020 ·
Published Online: 29 June 2020

View Online Export Citation CrossMark

Feng He,[1,2,a)] Emily S. Walker,[3] Yongjian Zhou,[1] Sarah E. Muschinske,[3] Seth R. Bank,[3] and Yaguo Wang[1,2,a)]

AFFILIATIONS

[1]Department of Mechanical Engineering, The University of Texas at Austin, Austin, Texas 78712, USA
[2]Texas Materials Institute, The University of Texas at Austin, Austin, Texas 78712, USA
[3]Microelectronics Research Center and Department of Electrical and Computer Engineering, The University of Texas at Austin, Austin, Texas 78758, USA

[a)]**Authors to whom correspondence should be addressed**: feng.he@utexas.edu and yaguo.wang@austin.utexas.edu

ABSTRACT

Coherent acoustic phonon dynamics in single-crystalline bismuth nanofilms transferred to a glass substrate were investigated with ultrafast pump–probe spectroscopy. Coherent phonon signals were substantially enhanced by more than four times when compared with as-grown films on Si (111) substrates. Furthermore, more than 10% reduction of the acoustic phonon velocity was observed when the film thickness decreases to 22 nm, which is attributed to the modified phonon dispersion in extremely thin films from quantum confinement effects.

Bismuth is an emerging quantum material with fascinating physical properties, such as semimetal–semiconductor (SM–SC) transition[1–8] and topological insulating states.[9–12] The development of the molecular beam epitaxy (MBE) growth technique has produced high quality Bi films in which rich physics theoretically predicted over the past five decades can be realized experimentally. Examples include, but are not limited to, exceptional surface-state spin and valley properties,[2,13] superconductivity,[14] transient high-symmetry phase transformation,[15] and anharmonic scattering.[16,17] In addition, the combination of a negative real part of the dielectric constant and a small imaginary part, as well as the strong inter-band transition, makes it promising for application in inter-band plasmonics.[18] Nevertheless, applications of single-crystalline Bi nanofilms in real devices are still limited by the fact that they can only be grown on lattice-matched substrates, such as silicon (111),[19] BaF_2 (111),[20] and mica.[21] Recently, Walker *et al.* introduced a double cantilever beam fracture[8,22] and thermal-release tape[23] technique for the dry transfer of large-area MBE Bi nanofilms from Si (111) to arbitrary substrates; they also showed that the electrical/optical/structural properties of the transferred films were comparable to the as-grown films.[8,23] This technique enables the study of the unique electronic, phononic, and spintronic properties of Bi on arbitrary substrates, such as transparent, flexible, magnetic, or topologically insulating ones for emerging devices. Most previous studies of coherent phonons in bismuth focused on optical phonons[15–17,24–28] and typically employed polycrystalline films prepared by thermal deposition. In this study, we have employed ultrafast pump–probe measurements to measure coherent acoustic phonons (CAPs) in transferred single-crystalline bismuth nanofilms[29] and examined the effect of quantum confinement on CAP dynamics. Our results show greatly enhanced CAP signals in single-crystalline Bi nanofilms transferred onto glass and a substantially reduced sound velocity when the thickness was reduced to <30 nm. The strong quantum confinement effects observed here could enable high-performance thermoelectrics[30,31] as an alternative to the notable Bi_2Te_3 and advanced acousto-optic devices[32] based on transferred epitaxial Bi nanofilms.

Single-crystalline bismuth nanofilms oriented in the [001] hexagonal direction (alternatively defined as [111] rhombohedral) with thicknesses between 20 and 50 nm were grown on a Si (111) substrate through MBE and then transferred to the glass substrate through a direct dry transfer method (see Fig. S1 in the supplementary material), which has not been achieved for bismuth previously.[8] The thicknesses were measured by x-ray reflectivity (XRR) before and after transfer (see Fig. S2). A custom coherent phonon spectrometer was used to carry out the experiments, where laser pulses from a mode-locked Ti:sapphire femtosecond laser (Spitfire ACE, Spectra Physics, 800 nm

wavelength, 35 fs pulse duration, 5 kHz repetition rate) were implemented. For the pump beam, a second harmonic generation crystal (beta-barium borate, BBO) was used to double the photon energy to 3.1 eV. The absorption depth for bismuth at 400 nm is ~15 nm.[28] A 15 cm lens was used to focus the collinear pump and probe beams, with spot sizes (diameter at the $\frac{1}{e^2}$ intensity level) of 245 μm and 60 μm, respectively. The pump fluence was fixed at 1.08 mJ/cm^2. All devices were synchronized through computer control for real-time data acquisition.[33–35]

By using the two-color pump–probe technique, we have measured the transient differential reflectivity change for four transferred bismuth nanofilms on glass and two reference as-grown bismuth nanofilms on Si (111), all at a fixed pump fluence of 1.08 mJ/cm^2. The absorption depth for the pump is ~15 nm and for the probe is ~15 nm,[27] which is on the order of the thicknesses (L) we measured; thus, we can get interference (coherent oscillations) pattern to extract our coherent phonon sound velocity through $v_{LA} = 2Lf_0$, where f_0 is the fitting frequency from the interference signal. On the other hand, if the sample thickness is much larger than the absorption depth, we will then get an echo-like coherent phonon signal, like Ref. 36, and we will extract the sound velocity through $v_{LA} = 2L/t$, where t is the round trip delay time. From the long delay time measurement, as shown in Fig. 1, we could observe that in the samples with a film thickness of above 30 nm, the $\Delta R/R$ first experienced an increase within the first 1 ps and then decreased to negative values with a slow recovery to the equilibrium afterwards. By contrast, the signal was always negative in the film with a thickness of 22.6 nm. Oscillations in the transient reflectivity change arise due to interference between the reflected probe beam at the air/Bi interface and the CAP-modulated reflected probe beam at the Bi/substrate interface. In the as-grown Bi/Si samples, it is hard to observe any oscillation signals, while in the transferred Bi/glass samples, the oscillations have large amplitudes. From Fig. 1(a), we can barely see any oscillations in the 55.2 nm Bi/Si sample and with four times amplification for the oscillation signal in a 42 nm Bi/Si sample; as shown in the inset of Fig. 1(b), we can see a comparable oscillation amplitude with that in a 42 nm Bi/Glass sample. As shown in Fig. 2(a), we have finer measurements of the Bi/glass samples using a time resolution of 1.6 ps in the shorter time window. We can observe the first dip within 20–25 ps, indicating the emergence of CAP. The delay time before the first dip decreases with a decreasing film thickness, as provided by the green arrow for eye guidance. The dashed line indicates the dip at 14.4 ps for the bismuth film with a thickness of 22.6 nm. We have plotted this appearance time for the first dip as a function of film thickness, and we find that it is not linearly dependent on the thickness [see Fig. 2(b)]. This will be discussed shortly.

For optically thin films with thickness smaller or comparable to the light penetration depth, the total reflection from the film is determined by both the real (n) and imaginary (κ) parts of the refractive index ($\sim n = n - i\kappa$). The total reflection is actually the interference of multiple light beams that reflected from the air/film interface and from the film/substrate interface, as well as the beams bounced between these two interfaces for several more times. To better understand the origin of the sign change within the first 1 ps, we have applied the transfer matrix method to simulate the impact on the $\Delta R/R$ signal from the perturbation of the real part n and imaginary part k of the refractive index for different thicknesses.[37] Our simulated results (see Fig. S3) show that below 30 nm, the magnitude of n and k does not change much, while the slope of k changes from negative to positive, indicating that the sign difference may mostly come from the refractive index change due to a short sample thickness, which is smaller or comparable to the optical absorption depth. Upon the arrival of the ultrafast pulse at the Bi surface, due to large electron–phonon (e–ph) coupling in Bi, CAP will be launched through the thermoelastic effect, where lattice anharmonicity enables thermal

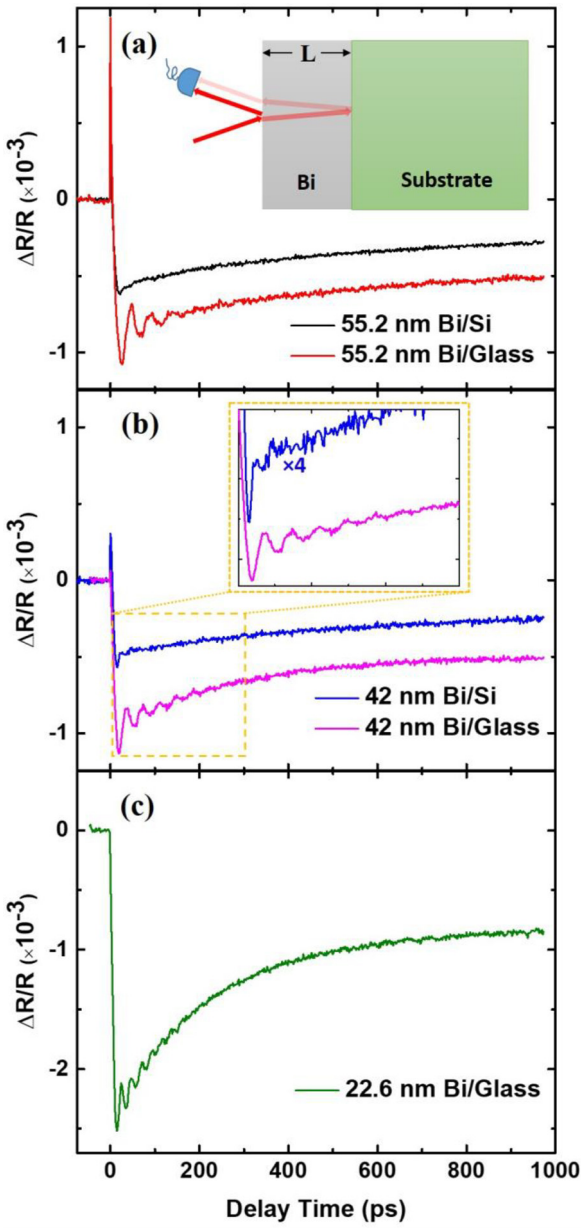

FIG. 1. Transient reflectivity change of bismuth nanofilms with a thickness of (a) 55.2 nm on the silicon substrate and glass substrate. Inset: the schematic of detection geometry in the Bi nanofilm/substrate system; (b) 42 nm on the silicon substrate and glass substrate. A zone-in figure displays the comparison of the oscillations before 300 ps as shown in the inset, and the oscillations in 42 nm Bi/Si are multiplied by a factor of 4 to show a comparable amplitude with that in 42 nm Bi/glass; and (c) 22.6 nm on glass substrate. All measurements were taken at the fluence of 1.08 mJ/cm^2.

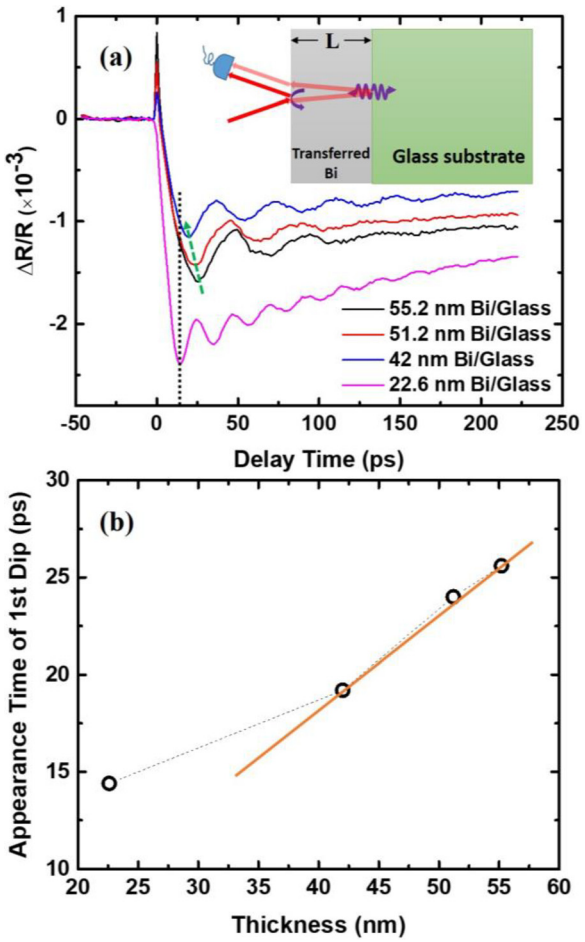

FIG. 2. (a) Transient reflectivity change of bismuth thin films on the glass substrate at the fluence of 1.08 mJ/cm^2. The green arrow provides the eye guidance for the dip shifting to the shorter delay time with decreasing thickness, and the dashed line indicates the dip at 14.4 ps for a 22.6 nm bismuth film. Inset: the schematic of generation and detection of CAP in the Bi/glass: red arrows are the probe light and purple arrows are the CAPs; the interference between the reflected probe beam from the surface and the CAP modulated probe beam is recorded by the detector; and (b) the appearance time for the first dip as a function of the film thickness (the orange line is a linear line for eye guidance).

expansion, similarly to the typical mechanism in metals.[38] However, Shin mentioned that in such thin films, the hot carriers will distribute evenly throughout the film, and thus uniform lattice temperature will be raised via e–ph coupling.[27,39] This suggests that no generation of acoustic pulse over the film is possible through volume expansion. Therefore, the non-uniform thermal expansion happens at the Bi/glass interface [as shown in Fig. 2(a)] due to the thermal gradient at the interface.[40] The appearance of the first dip around 20 ps and the time shift of this dip at different thicknesses further prove the generation of the CAPs at the Bi/glass interface. The CAPs are partially reflected, propagating backward, and finally arrive at the surface around 20 ps. The modulation of the local refractive index induced by the CAPs modulates the reflected probe beam from the Bi/substrate interface through the photoelastic effect. Therefore, there are two possible reasons for the disappearance of the CAP signal in the Bi/Si of the thicknesses around 40–50 nm: (i) the thermal gradient across the Bi/Si interface is weak compared with that of the Bi/glass interface, leading to a smaller amplitude of the CAP generated through the thermoelastic effect; (ii) the reflected CAP at the Bi/Si interface is too weak to detect due to the "magic mismatch" between the Bi (001) phase and the Si (111) surface,[19] even though the lattice mismatch between the Bi (001) and Si (111) is ∼18%. Whereas, in the transferred Bi/glass samples, the CAP signal is substantially enhanced both because of a large acoustic impedance difference and the real part of the refractive index difference between Bi and glass, where the values of acoustic impedance for Si, Bi, and glass are 2.13×10^7 Pa s/m, 2.16×10^7 Pa s/m, and 1.41×10^7 Pa s/m, respectively. Our results show more pronounced oscillations than were observed by Shin in the Bi/silica glass samples prepared by sputtering deposition,[39] indicating the presence of abrupt interfaces in our transferred nanofilms on glass. This large coherent acoustic phonon signal enables the opportunity to study the thickness effects on the transferred film with different substrates.

A very interesting phenomenon we can observe from Fig. 2 is that the appearance of the first dip at 14.4 ps in the 22.6 nm Bi/glass and at 19.2 ps in the 42 nm Bi/glass suggests a smaller sound velocity in the 22.6 nm film than in the 42 nm film. To better investigate this phenomenon, we have extracted the sound velocity for different film thicknesses. We eliminated the signal from electron excitation and recombination and the non-oscillating background by using the smoothing function (adjacent-averaging) in software and fitted the oscillating part with the Eq. (1) (see Fig. S3)

$$\frac{\Delta R}{R} = A\exp\left(-t/\tau_p\right)\cos(2\pi f t + \phi_0), \tag{1}$$

$$f = f_0 + \beta t, \tag{2}$$

where A, τ_p, f_0, β, and ϕ_0 are the amplitude, the dephasing time, the initial frequency, the linear chirp rate, and the initial phase, respectively. f is the transient phonon frequency and f_0 is the initial acoustic phonon frequency. By estimating the sound velocity using $v_{LA} = 2Lf_0$, where L is the bismuth film thickness measured with XRR and f_0 is extracted from the fitting, as shown in Fig. 3, we plot the sound velocity values as a function of film thickness in Fig. 4.

Overall, the extracted sound velocity in four different nanofilms is higher than the reported longitudinal acoustic (LA) phonon velocity along the [001] direction in the bulk.[39,41,42] Above 40 nm, the sound velocity is almost a constant around 2400 m/s, yet when the film is thinner than 30 nm, the sound velocity is substantially reduced by a reduction ratio of 10.9% ± 1.6%. In the literatures, there are a large range of values for bulk sound velocity in the [001] direction in bismuth, ranging from 1541 m/s to 1970 m/s, and the most commonly used one is 1790 m/s.[39,41,42] Therefore, we think the sound velocity might also be dependent on the samples. In our samples, the bulk value should be about 2400 m/s along the [001] direction. The decreased sound velocity in the 55 nm sample should still be within the error (see Fig. S4 considering the uncertainty of the measured thickness) except any interesting phenomenon showing up since combined with Fig. 2(b), where the time for the first dip (when the CAP, which was generated at the interface, arrived at the surface) is relatively linear for the thicknesses above 40 nm and the uncertainty for the delay time in our system is smaller than our resolution (1.6 ps) in this measurement.

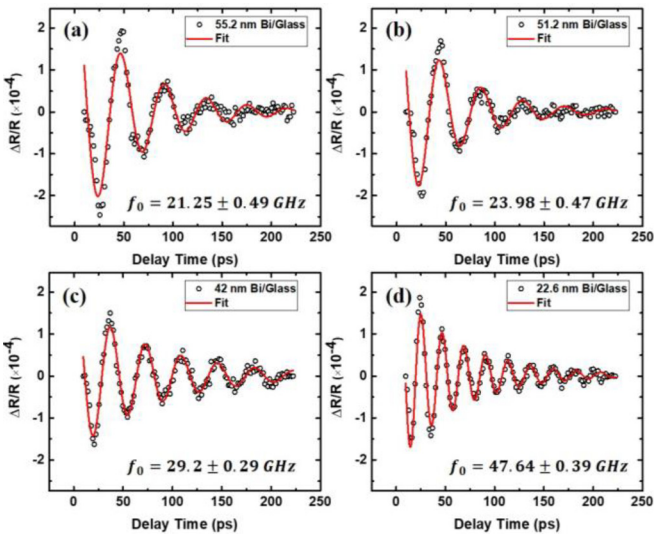

FIG. 3. Fitting results from Eq. (1) for four different thicknesses: (a) 55.2 nm, (b) 51.2 nm, (c) 42 nm, and (d) 22.6 nm. The fitted f_0 are (a) 21.25 ± 0.49 GHz, (b) 23.98 ± 0.47 GHz, (c) 29.2 ± 0.29 GHz, and (d) 47.64 ± 0.39 GHz, respectively. The black empty dots are the experiment data and the red solid line are the fittings.

This is consistent with the previous reports of reduced sound velocity in thinner films. Previously, Bonello *et al.* reported the reduction of the sound velocity in Cu/W multilayers, which was explained as the softening of the elastic constant related to the interfacial effects.[43] Wang *et al.* reported the sound velocity reduction in the Bi_2Te_3/Sb_2Te_3 superlattices with thinner periods due to flattened phonon dispersion.[36] Shin reported that a slower speed of acoustic pulse at

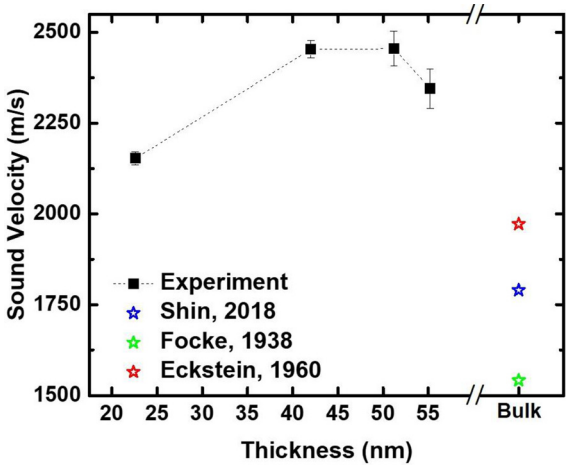

FIG. 4. Extracted sound velocity for four bismuth thin films with different thicknesses. The error bars show the uncertainty from fitting in Fig. 3. The empty stars are the reported speed of sound for bulk Bi along [001].[39,41,42] Reprinted with permission from T. Shin, Thin Solid Films **666**, 108 (2018).[39] Copyright 2018, Elsevier; Reprinted with permission from Focke *et al.*, J. Acoust. Soc. Am. **9**, 348 (1938).[41] Copyright 1938 Acoustical Society of America; Reprinted with permission from Eckstein *et al.*, J. Appl. Phys. **31**, 1534 (1960).[42] Copyright 1960 AIP Publishing LLC.

a higher pump fluence occurs in the 38 nm bismuth film because of the lattice bond softening at elevated temperatures.[39] However, the bond softening due to higher temperatures should not be the reason in our case since according to the estimation of the average density throughout the film,[27] under the fluence of 1.08 mJ/cm^2 in our case, the photoexcited carrier densities are 1.3×10^{19}/cm^3 for 42 nm and 2.4×10^{19}/cm^3 for 22.6 nm films. In addition, the average temperature is estimated as 360 K for 42 nm and 414 K for 22.6 nm films, smaller temperature differences (54 K) than Shin reported (155 K), while the time difference is larger (4.8 ps compared to 3 ps).[39]

As the thickness of the material shrinks, different confined acoustic phonon branches can emerge as a result of the spatial confinement, such as that shown in the silicon thin film.[44] However, our experiment could only detect a narrow spectrum of longitudinal acoustic (LA) modes along the [001] direction near the first Brillouin center, limited by both the phonon generation mechanism via Brillouin scattering and our experiment geometry (normal incidence with pump/probe size ratio ~4). The characteristic length to observe the phonon confinement is a key parameter. When considering the quantum confinement effects for the thermally important phonons, which are usually in THz range, the phonon gray mean free path (MFP) can be a good choice.[45] However, for the low frequency phonons, this characteristic length can be much longer than MFP. Cuffe *et al.* found a reduction of the sound velocity of the fundamental flexural mode (in GHz range) in ultrathin Si membranes up to 143 nm, much larger than the Si average phonon MFP (~40 nm).[46] Kargar *et al.* have also shown that the confinement of GHz phonons can happen in GaAs nanowires with a diameter of up to 128 nm, much larger than GaAs phonon MFP (~20 nm).[47] Moreover, Johnson *et al.* proposed the "medium thermal conductivity MFP," which appears to be a more useful parameter in analyzing the onset of the size effects in thermal conductivity than the phonon gray MFP.[48] For Bi, the estimated gray MFP is around 11 nm, which means confinement effects of many thermal phonons could occur when the sample thickness is comparable or less than 11 nm. All our sample thicknesses are much larger than 11 nm. While in our experiment, the measured CAPs are in the range of 20–50 GHz and has a wavelength up to 144 nm. As a result, we only observed the confinement effect for the detected CAPs. Hence, our findings agree with the previous studies, in that the quantum confinement of low frequency phonons could occur at a thickness much larger than gray MFP. While modified phonon dispersions have been reported by several groups in superlattice structures, where the phonon dispersion is modified by the periodicity, a similar effect in thin films has only been reported in a few studies. In 1997, Gaganidze *et al.* reported a strong effect of film thickness and substrate temperature on the sound velocity maximum in SiO_2 films at extremely low temperatures. They attributed this phenomenon to a modification of the phonon mediated interaction between the tunneling system due to the smaller dimensionality.[49] This suggests that in very thin films, the phonon dispersion can also be modified by the dimensional confinement, similar to the quantum confinement of electrons. In addition, by calculating the dispersion relation of the acoustic phonon propagating in both bulk and membrane Si, Volz *et al.* found that in the membrane Si, the phonon dispersion was modified and group velocity at smaller wavevectors was reduced.[50] Therefore, the reduced velocity in the 22 nm Bi film in our case is likely to be mainly caused by the flattened phonon dispersion introduced by quantum confinement. The single-crystalline

nature of the Bi helps to manifest this phenomenon, since in the polycrystalline Bi, the mixed crystal directions may account for the suppression of this effect. Moreover, we observe that with thinner films, less uncertainty is obtained in the measurement of Bi/glass, contributing from the more round trips of the CAP recorded, as well as less loss of the probe beam in the thinner films.

In conclusion, we have employed a noncontact and nondestructive ultrafast pump–probe spectroscopy to investigate CAP dynamics in single-crystalline epitaxial bismuth nanofilms transferred to the glass substrates. Comparing with the as-grown nanofilms on silicon substrates, our results show greatly enhanced CAP signals in the transferred Bi nanofilms on glass, benefiting from the difference in the acoustic impedance and real part of the refractive index between Bi and glass. We also find a more than 10% reduction of sound velocity for films thinner than 30 nm, where the flattened phonon dispersion induced by the strong quantum confinement effect of high-quality Bi nanofilms is one of the possible reasons. It is interesting to note that the sound velocity reduction occurs concomitantly with the predicted SM–SC transition,[1–8] when the surface state transport begins to dominate over the bulk transport. This merits further study into the effect of quantum confinement, which drives the SM–SC transition, on phonon dynamics in Bi. This study suggests the potential of transferred epitaxial Bi nanofilms for applications in high-performance thermoelectrics and acousto-optic devices.

See the supplementary material for the sample preparation and XRR data for samples, as well as the propagation of errors.

The authors acknowledge support from the National Science Foundation (NASCENT, Grant No. EEC-1160494; CAREER, Grant No. CBET-1351881; No. CBET-1707080; and Center for Dynamics and Control of Materials No. DMR-1720595).

DATA AVAILABILITY

The data that support the findings of this study are available within the article and its supplementary material.

REFERENCES

[1]S. Xiao, D. Wei, and X. Jin, Phys. Rev. Lett. **109**, 166805 (2012).
[2]N. Marcano, S. Sangiao, C. Magen, L. Morellón, M. R. Ibarra, M. Plaza, L. Pérez, and J. D. Teresa, Phys. Rev. B **82**, 125326 (2010).
[3]M. Lu, R. Zieve, A. Van Hulst, H. Jaeger, T. Rosenbaum, and S. Radelaar, Phys. Rev. B **53**, 1609 (1996).
[4]B. Halperin and T. Rice, Rev. Mod. Phys. **40**, 755 (1968).
[5]V. Lutskii and L. Kulik, "Features of optical characteristics of bismuth films under conditions of quantum size effect," Zh. Eksp. Teor. Fiz. Pis'ma Red. **8**(3), 133–137 (1968).
[6]C. Hoffman, J. Meyer, F. Bartoli, A. Di Venere, X. Yi, C. Hou, H. Wang, J. B. Ketterson, and G. Wong, Phys. Rev. B **48**, 11431 (1993).
[7]V. Sandomirskii, "Quantum size effect in a semimetal film," Sov. Phys. JETP **25**(1), 101–106 (1967).
[8]E. S. Walker, S. R. Na, D. Jung, S. D. March, J.-S. Kim, T. Trivedi, W. Li, L. Tao, M. L. Lee, and K. M. Liechti, Nano Lett. **16**, 6931–6938 (2016).
[9]L. Chen, Z. Wang, and F. Liu, Phys. Rev. B **87**, 235420 (2013).
[10]I. K. Drozdov, A. Alexandradinata, S. Jeon, S. Nadj-Perge, H. Ji, R. J. Cava, B. A. Bernevig, and A. Yazdani, Nat. Phys. **10**, 664 (2014).
[11]C.-H. Hsu, X. Zhou, T.-R. Chang, Q. Ma, N. Gedik, A. Bansil, S.-Y. Xu, H. Lin, and L. Fu, Proc. Natl. Acad. Sci. **116**, 13255–13259 (2019).
[12]F. Schindler, Z. Wang, M. G. Vergniory, A. M. Cook, A. Murani, S. Sengupta, A. Y. Kasumov, R. Deblock, S. Jeon, I. Drozdov, H. Bouchiat, S. Guéron, A. Yazdani, B. A. Bernevig, and T. Neupert, Nat. Phys. **14**, 918–924 (2018).
[13]H. Du, X. Sun, X. Liu, X. Wu, J. Wang, M. Tian, A. Zhao, Y. Luo, J. Yang, and B. Wang, Nat. Commun. **7**, 10814 (2016).
[14]O. Prakash, A. Kumar, A. Thamizhavel, and S. Ramakrishnan, Science **355**, 52 (2017).
[15]S. W. Teitelbaum, T. Shin, J. W. Wolfson, Y.-H. Cheng, I. J. Porter, M. Kandyla, and K. A. Nelson, Phys. Rev. X **8**, 031081 (2018).
[16]M. Hase, M. Kitajima, S.-I. Nakashima, and K. Mizoguchi, Phys. Rev. Lett. **88**, 067401 (2002).
[17]S. W. Teitelbaum, T. Henighan, Y. Huang, H. Liu, M. P. Jiang, D. Zhu, M. Chollet, T. Sato, É. D. Murray, S. Fahy, S. O'Mahony, T. P. Bailey, C. Uher, M. Trigo, and D. A. Reis, Phys. Rev. Lett. **121**, 125901 (2018).
[18]J. Toudert and R. Serna, Opt. Mater. Express **7**, 2299 (2017).
[19]T. Nagao, J. Sadowski, M. Saito, S. Yaginuma, Y. Fujikawa, T. Kogure, T. Ohno, Y. Hasegawa, S. Hasegawa, and T. Sakurai, Phys. Rev. Lett. **93**, 105501 (2004).
[20]D. Partin, J. Heremans, D. Morelli, C. Thrush, C. Olk, and T. Perry, Phys. Rev. B **38**, 3818 (1988).
[21]N. Garcia, Y. Kao, and M. Strongin, Phys. Rev. B **5**, 2029 (1972).
[22]S. R. Na, J. W. Suk, L. Tao, D. Akinwande, R. S. Ruoff, R. Huang, and K. M. Liechti, ACS Nano **9**, 1325 (2015).
[23]S. E. Muschinske, E. S. Walker, S. R. Na, S. D. March, A. F. Briggs, D. Akinwande, K. J. Liechti, and S. R. Bank, paper presented at the 59th Electronic Materials Conference (EMC), South Bend, IN, 2017.
[24]M. Hase, K. Mizoguchi, H. Harima, S.-I. Nakashima, and K. Sakai, Phys. Rev. B **58**, 5448 (1998).
[25]D. M. Fritz, D. Reis, B. Adams, R. Akre, J. Arthur, C. Blome, P. Bucksbaum, A. L. Cavalieri, S. Engemann, and S. Fahy, Science **315**, 633 (2007).
[26]K. Ishioka, M. Kitajima, O. V. Misochko, and T. Nagao, Phys. Rev. B **91**, 125431 (2015).
[27]T. Shin, J. W. Wolfson, S. W. Teitelbaum, M. Kandyla, and K. A. Nelson, Phys. Rev. B **92**, 184302 (2015).
[28]A. Q. Wu and X. Xu, Appl. Phys. Lett. **90**, 251111 (2007).
[29]J. A. Rogers, A. A. Maznev, M. J. Banet, and K. A. Nelson, Annu. Rev. Mater. Sci. **30**, 117 (2000).
[30]H. Goldsmid, paper presented at the 2006 25th International Conference on Thermoelectrics, IEEE, 2006.
[31]L. Hicks and M. S. Dresselhaus, Phys. Rev. B **47**, 12727 (1993).
[32]H. Ding, X. Shu, Y. Jin, T. Fan, and H. Zhang, Nanoscale **11**, 5839–5860 (2019).
[33]F. He, W. Wu, and Y. Wang, Appl. Phys. A **122**, 777 (2016).
[34]W. Wu, F. He, and Y. Wang, J. Appl. Phys. **119**, 055701 (2016).
[35]F. He, N. Sheehan, S. R. Bank, and Y. Wang, Opt. Lett. **44**, 4590 (2019).
[36]Y. Wang, C. Liebig, X. Xu, and R. Venkatasubramanian, Appl. Phys. Lett. **97**, 083103 (2010).
[37]C. C. Katsidis and D. I. Siapkas, Appl. Opt. **41**, 3978 (2002).
[38]P. Ruello and V. E. Gusev, Ultrasonics **56**, 21 (2015).
[39]T. Shin, Thin Solid Films **666**, 108 (2018).
[40]O. Wright, J. Appl. Phys. **71**, 1617 (1992).
[41]A. Focke, R. Lindsay, and C. Wilks, J. Acoust. Soc. Am. **9**, 348 (1938).
[42]Y. Eckstein, A. Lawson, and D. H. Reneker, J. Appl. Phys. **31**, 1534 (1960).
[43]B. Bonello, B. Perrin, E. Romatet, and J. Jeannet, Ultrasonics **35**, 223 (1997).
[44]A. A. Balandin and D. L. Nika, Mater. Today **15**, 266 (2012).
[45]M. N. Luckyanova, J. Garg, K. Esfarjani, A. Jandl, M. T. Bulsara, A. J. Schmidt, A. J. Minnich, S. Chen, M. S. Dresselhaus, and Z. Ren, Science **338**, 936 (2012).
[46]J. Cuffe, E. Chavez, A. Shchepetov, P.-O. Chapuis, E. H. El Boudouti, F. Alzina, T. Kehoe, J. Gomis-Bresco, D. Dudek, and Y. Pennec, Nano Lett. **12**, 3569 (2012).
[47]F. Kargar, B. Debnath, J.-P. Kakko, A. Säynätjoki, H. Lipsanen, D. L. Nika, R. K. Lake, and A. A. Balandin, Nat. Commun. **7**, 1 (2016).
[48]J. A. Johnson, A. A. Maznev, J. Cuffe, J. K. Eliason, A. J. Minnich, T. Kehoe, C. M. S. Torres, G. Chen, and K. A. Nelson, Phys. Rev. Lett. **110**, 025901 (2013).
[49]E. Gaganidze, R. König, P. Esquinazi, K. Zimmer, and A. Burin, Phys. Rev. Lett. **79**, 5038 (1997).
[50]S. Volz, J. Ordonez-Miranda, A. Shchepetov, M. Prunnila, J. Ahopelto, T. Pezeril, G. Vaudel, V. Gusev, P. Ruello, and E. M. Weig, Eur. Phys. J. B **89**, 15 (2016).